Supporting Information

Ebert et al. 10.1073/pnas.1502390112

SI Materials and Methods

HBV Plasmid. The plasmid (pAAV-HBV1.2) for hydrodynamic injection contains a 1.2 over length HBV genome spanning nucleotides 1,400–3,182/1–1,987 flanked by inverted terminal repeats of an adeno-associated virus (1). The plasmid contains the coding sequence for HBV genotype A, serotype adw. Plasmid pAAV-HBV1.2 was prepared using the EndoFree Plasmid Maxi Kit (Qiagen).

Mice. The Walter and Eliza Hall Institute of Medical Research Animal Ethics Committee reviewed and approved all animal experiments. Animals used in experiments were between 6 and 10 wk old, and they were age- and sex-matched (both sexes were used). The gene-targeted animals used in our experiments have been described elsewhere (2–10). We crossed the relevant single-mutant animals to generate compound mutant cIAP1$^{\Delta Hep/\Delta Hep}$ cIAP2$^{-/-}$ mice. All mice, apart from the C3H strain, were on a C57BL/6 background, including gene-targeted animals. Chimeric mice were generated by harvesting fetal liver cells from congenic mice of the specified genotypes and transferring these cells to irradiated congenic recipients with the indicated genotype as previously described (11).

Hydrodynamic Injection. Unanesthetized mice were injected i.v. through the tail vein with 10 μg pAAV-HBV1.2 in a volume of saline equivalent to 8% of the mouse body weight. The injection was performed within 5 s.

LCMV Infection. Six-week-old C57BL/6 mice were injected with 3×10^3 pfu LCMV Armstrong strain or 2×10^6 pfu LCMV Docile strain through the tail vein.

In Vivo Antibody Administration. The following doses of antibodies were administered i.p. at the specified times: 100 μg rat IgG2b anti-CD4$^+$ (GK1.5–1), 100 μg rat IgG2b anti-CD8$^+$ (YTS-169), 200 μg rat IgG1 anti-TNF (XT-22), 200 μg rat IgG1 isotype control, 200 μg mouse IgG1 anti–IFNAR-1 (MAR1-5A3), and 200 μg mouse IgG1 isotype control (GIR-208).

Serum HBV DNA Quantification. Viral DNA was extracted from serum using the High Pure Viral Nucleic Acid Kit (Roche) or the Invisorb Virus DNA HTS 96 Kit (Stratec). Quantification was performed using real-time RT-PCR and the DNA Amplification SYBR Green Kit (Roche) on a LightCycler 480 II Machine (Roche) with Absolute Quantification Software (Roche). Serial dilutions of pAAV-HBV1.2 were used as the standard. Primers were HBV1745fw (GTTGCCCGTTTGTCCTCTAATTC) and HBV1844rev (TGAGGGAAACATAGAGTTGCCTTGA). Our limit of detection of serum HBV DNA was 500 copies/mL.

Plasmid Backbone Quantification in Liver. Livers were thoroughly perfused in situ with PBS to remove blood. Total liver DNA was extracted using the DNeasy Blood and Tissue Kit (Qiagen) according to the manufacturer's instructions. The plasmid backbone DNA was quantified by real-time PCR using primers specific for the plasmid backbone of pAAV-HBV1.2 that do not bind to HBV sequences. Primers were bb439fw (AAGGCCGATAGTTTGAGTTC) and bb851rev (GGAGCCCCCGATTTAGA). Serial dilutions of pAAV-HBV1.2 were used as a standard. A standard of 10^5 copies is shown.

HBV Genome Quantification in Liver. Total liver DNA extraction was as described above for plasmid backbone quantification. We quantified liver HBV genome expression by real-time PCR using primers HBV1745fw and HBV1844rev relative to GAPDH expression using the DNA Amplification SYBR Green Kit (Roche) and a LightCycler 480 II Machine (Roche) with Relative Quantification Software (Roche).

HBV Serology and Aspartate Aminotransferase/Alanine Aminotransferase Quantification. Quantification of serum HBsAg, HBeAg, anti-HBV antibody, and transaminases was performed using a Cobas e411 Analyzer (Roche) per the manufacturer's instructions.

Immunofluorescence. Livers were perfused ex vivo with 2% paraformaldehyde and fixed for another 4 h at 4 °C. Fixed livers were dehydrated in 30% sucrose for 16 h, embedded in Tissue-Tek Optimal Cutting Temperature (Sakura Finetek) media, and frozen rapidly using liquid N_2. Immunostaining was performed on 8-μm cryosections of livers on poly-L-lysine glass slides. Thawed slides were dried and postfixed for 20 min using ice-cold acetone. Slides were washed using PBS and blocked with a solution of 5% goat serum (Abcam) in PBS for 30 min at room temperature. Slides were stained for 1 h with primary antibodies targeting either HBcAg (rabbit anti-HBcAg; 1:200; Dako) or MHC class Ia [rat anti–H-2k^b, phycoerythrin (PE)-conjugated; 1:100; BD]. For HBcAg staining, slides were stained for 30 min with a secondary antibody (goat anti-rabbit AF594-conjugated; 1:1,000; Molecular Probes). Slides were washed three times with PBS between each staining. Coverslips were mounted using ProLong Gold Antifade containing DAPI (Molecular Probes) for 16 h at 4 °C. Slides were visualized on a Zeiss AxioObserver. Z1 Confocal Microscope (Carl Zeiss Microsystems) with a 20× N.A. dry objective. The numbers of HBcAg-positive hepatocytes and hepatic nuclei were counted for five to eight random fields (~2,200 hepatocytes per field) per liver.

TUNEL Assay. The TUNEL reaction was performed on cryosections using the DeadEnd Flurogenic Tunel Kit (Promega) and counterstained with allophycocyanin (APC)–streptavidin (1:200; Molecular Probes) in PBS. Coverslips were mounted, and slides were imaged as described previously.

Immunophenotyping of Hepatic Immune Cells. After PBS perfusion, one-third of the whole liver was taken, and immune cells were isolated after liver disruption with a 100-μm mesh filter and Percoll (GE Healthcare) gradient centrifugation. Approximately 10^6 cells were strained for 1 h at 4 °C in PBS supplemented with 2% FCS (Sigma) with fluorochrome-conjugated antibodies against CD8 (PeCy7; clone 53–6.7; BD Biosciences), CD4 (MCD0427; APC Alexa Fluor 750; Invitrogen), CD44 (V500; clone IM7; BD Biosciences), CD62L (APC; clone MEL-14; BD Biosciences), PD1 (PE; clone J43; BD Biosciences), and CD69 (BV421; clone H1.2F3; BD Biosciences). Data were acquired using a Fortessa ×20 Flow Cytometer (BD Biosciences) and analyzed with FacsDIVA Software (BD Biosciences). For ex vivo restimulation assays, T cells were isolated as described above, and then, they were plated and stimulated with phorbol myristate acetate and ionomycin. After stimulation, cells were sequentially surface-stained, fixed, and permeabalized for intracellular cytokine staining as described previously (12).

Northern Blots. Total RNA was isolated from 50 mg liver tissue using TRIzol (Invitrogen) according to the manufacturer's instructions. Approximately 30 μg per lane total mouse liver RNA was resolved using a 1% agarose gel and transferred onto a

positively charged nylon membrane using the NorthernMax Gly Kit (Ambion) according to the manufacturer's instructions. A generated probe was labeled with DIG dUTP by PCR using the PCR digoxigenin (DIG) Probe Synthesis Kit (Roche) and primers 2,954 (atatgaacctttaccccgttgc) and PC2 (ggcaaaaacgagagtaactc). Blots were hybridized with DIG Easy Hyb (Roche) according to the manufacturer's instructions, and immunological detection of DIG-labeled probes was performed as per manufacturer's instructions using the DIG Wash and Block Buffer Set, anti-digoxigenin-AP, Fab fragments, and CDP-Star (Roche). ECL images were obtained using ChemiDoc XP instrumentation and Image Lab software (Bio-Rad).

Western Blots. Total liver protein lysates were prepared from 25 mg liver tissue that was homogenized in cell lysis buffer containing 20 mM Tris·HCl, pH 7.5, 135 mM NaCl, 1.5 mM Mg_2Cl, 1 mM EGTA, 1% Triton X-100 (Sigma-Aldrich), 10% Glycerol (Ajax Finechem), EDTA-free protease inhibitor mixture tablets, and phosphatase inhibitor mixture tablets (Roche) using a tissue homogenizer (Tissue Lyser II; Qiagen). Lysates (50 μg protein per lane) were separated using 4–12% SDS/PAGE. Proteins were transferred onto nitrocellulose membranes and detected using primary and secondary antibodies. Antibodies included anti-XIAP mAb (1:1,000; MBLI), rat anti-cIAP1 (1:500; WEHI), hamster anti-TNFR1 (1:1,000; mab430; R&D Systems), and rabbit anti–β-actin (1:3,000; Cell Signaling Technology).

1. Huang LR, Wu HL, Chen PJ, Chen DS (2006) An immunocompetent mouse model for the tolerance of human chronic hepatitis B virus infection. *Proc Natl Acad Sci USA* 103(47):17862–17867.
2. Pérarnau B, et al. (1999) Single H2Kb, H2Db and double H2KbDb knockout mice: Peripheral CD8+ T cell repertoire and anti-lymphocytic choriomeningitis virus cytolytic responses. *Eur J Immunol* 29(4):1243–1252.
3. Kägi D, et al. (1994) Cytotoxicity mediated by T cells and natural killer cells is greatly impaired in perforin-deficient mice. *Nature* 369(6475):31–37.
4. Dalton DK, et al. (1993) Multiple defects of immune cell function in mice with disrupted interferon-gamma genes. *Science* 259(5102):1739–1742.
5. Malissen M, et al. (1995) Altered T cell development in mice with a targeted mutation of the CD3-ε gene. *EMBO J* 14(19):4641–4653.
6. Spanopoulou E, et al. (1994) Functional immunoglobulin transgenes guide ordered B-cell differentiation in Rag-1-deficient mice. *Genes Dev* 8(9):1030–1042.
7. Schile AJ, García-Fernández M, Steller H (2008) Regulation of apoptosis by XIAP ubiquitin-ligase activity. *Genes Dev* 22(16):2256–2266.
8. Gardam S, et al. (2011) Deletion of cIAP1 and cIAP2 in murine B lymphocytes constitutively activates cell survival pathways and inactivates the germinal center response. *Blood* 117(15):4041–4051.
9. Postic C, et al. (1999) Dual roles for glucokinase in glucose homeostasis as determined by liver and pancreatic beta cell-specific gene knock-outs using Cre recombinase. *J Biol Chem* 274(1):305–315.
10. Barnden MJ, Allison J, Heath WR, Carbone FR (1998) Defective TCR expression in transgenic mice constructed using cDNA-based α- and β-chain genes under the control of heterologous regulatory elements. *Immunol Cell Biol* 76(1):34–40.
11. Pellegrini M, et al. (2005) FADD and caspase-8 are required for cytokine-induced proliferation of hemopoietic progenitor cells. *Blood* 106(5):1581–1589.
12. Pellegrini M, et al. (2009) Adjuvant IL-7 antagonizes multiple cellular and molecular inhibitory networks to enhance immunotherapies. *Nat Med* 15(5):528–536.

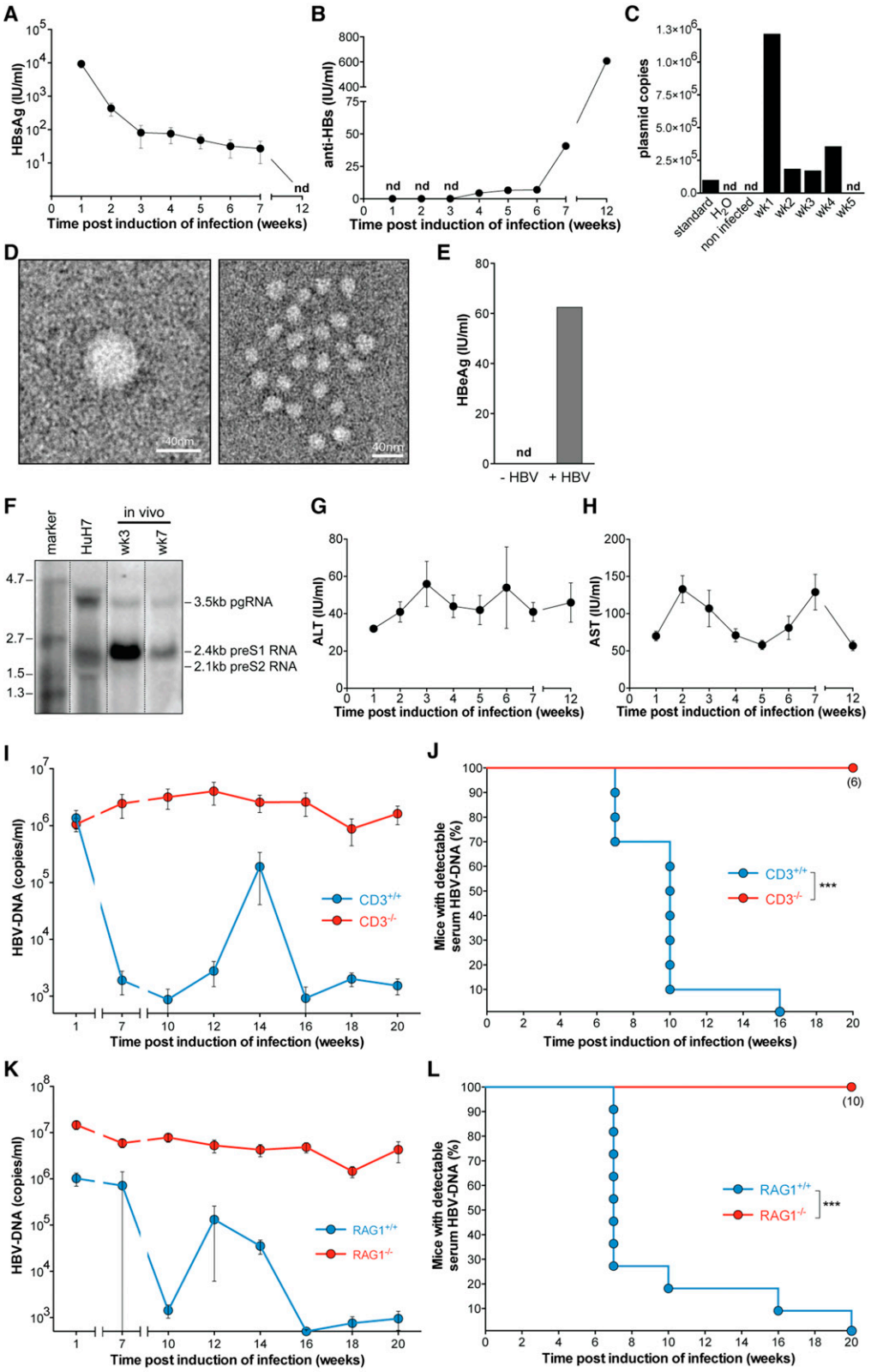

Fig. S1. Hydrodynamic injection model reproduces the human intracellular lifecycle of HBV in mice. (*A*) Serial measurement of serum HBsAg levels in HBV-infected C57BL/6 mice ($n = 10$). (*B*) Serum anti-HBV antibody levels in HBV-infected C57BL/6 mice at the indicated time points (n = pooled sera from 10 mice). (*C*) RT-PCR–quantifying plasmid backbone at the indicated times in livers of hydrodynamically injected C57BL/6 mice. (*D*) EM of serum from HBV-infected C57BL/6 mice 1 wk after induction of infection (n is the pooled sera from three animals). (*E*) Serum HBV e-antigen (HBeAg) levels in HBV-infected C57BL/6 mice 1 wk after induction of infection (n is the pooled sera from five mice). (*F*) Northern blot analysis of pre- and subgenomic HBV RNAs in the transfected HuH7 cell line expressing HBV and the livers from C57BL/6 mice infected with HBV at the indicated time points (representative of $n = 5$ mice at each time point).

Legend continued on following page

(*G* and *H*) Serum transaminases in C57BL/6 mice at the indicated time points after induction of HBV infection ($n = 10$). (*I*) Serial measurement of serum HBV DNA levels in mice of the indicated genotype after induction of HBV infection ($n = 6$–10 in each group). (*J*) Proportion of animals and time when mice with the specified genotypes first achieved an undetectable serum HBV DNA level ($n = 6$–10 for each group). (*K*) Serial measurement of serum HBV DNA levels in mice of the indicated genotype after induction of HBV infection ($n = 10$–11 in each group). (*L*) Proportion of animals and time when mice of the indicated genotypes first achieved an undetectable serum HBV DNA level ($n = 10$–11 for each group). Numbers below dots in time to event analyses represent remaining mice that have been censored. Graphs show means and SEMs, and data are representative of (*A*, *B*, *G*, and *H*) three or (*D*–*F* and *I*–*L*) two independent experiments that served as controls in the remainder of the study. (*A*, *B*, *E*, and *G*–*L*) Experiments were blinded. ALT, alanine aminotransferase; AST, aspartate aminotransferase; nd, not detected. ***$P < 0.001$ (log-rank Mantel–Cox test).

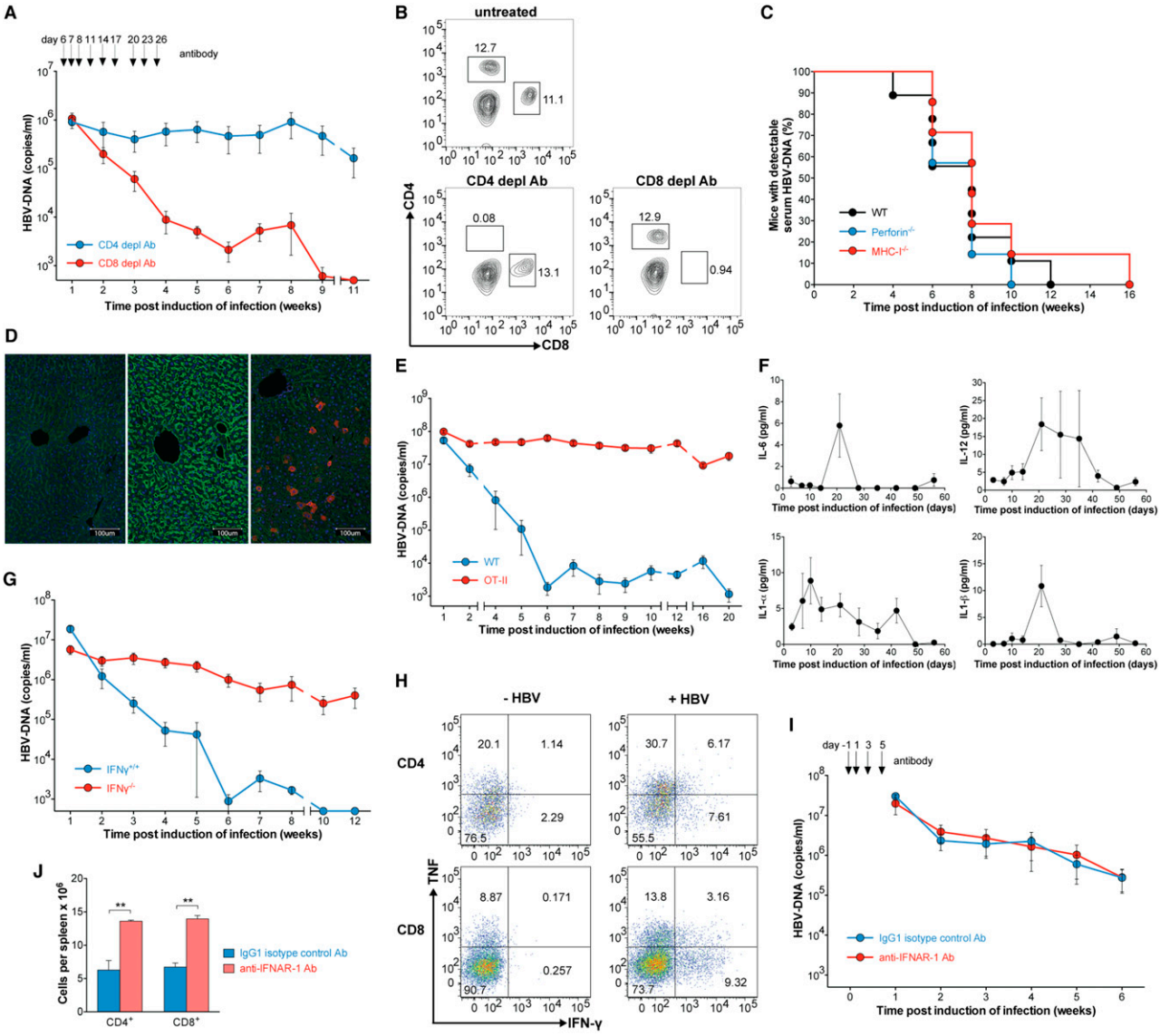

Fig. S2. $CD4^+$ T cells are critical for HBV control. (*A*) Serial measurement of serum HBV DNA levels in infected mice treated with the indicated antibodies at the times shown (arrows) after induction of infection ($n = 7–11$ in each group). (*B*) Flow cytometry analysis showing the proportion (number adjacent to boxes) of $CD4^+$ and $CD8^+$ cells in blood at day 21 during the T-cell depletion experiments described in *A*. (*C*) Proportion of animals and time when mice of the indicated genotypes first achieved an undetectable serum HBV DNA level ($n = 7–9$ for each group). (*D*) Immunofluorescence staining (blue, DAPI; green, MHC class I; red, HBcAg) of liver sections taken from (*Left*) uninfected mice, (*Center*) mice 2 d after LCMV infection, and (*Right*) mice during the height of HBV viremia 3 wk after induction of infection (representative of $n = 3$ per group). (*E*) Serial measurement of serum HBV DNA levels in infected mice with the specified genotypes ($n = 9–10$ in each group). (*F*) Serial quantification of serum cytokine levels at the indicated time points after induction of HBV infection in C57BL/6 mice ($n = 10$). (*G*) Serial measurement of serum HBV DNA levels in infected mice with the specified genotypes ($n = 7–10$ in each group). (*H*) Flow cytometry analysis showing proportion (number adjacent to boxes) of cytokine-producing $CD4^+$ and $CD8^+$ cells harvested from the livers of uninfected mice and mice 2 wk after induction of HBV infection. (*I*) Serial measurement of serum HBV DNA levels in infected C57BL/6 mice treated with the indicated antibodies at the times shown (arrows) starting 1 d before infection ($n = 5–6$ in each group). (*J*) Quantification of splenic T-cell numbers by flow cytometry at day 8 after chronic LCMV docile infection in mice treated with anti–IFNAR-1 Ab on days 3–5 postinfection. Graphs show means and SEMs, and data are representative of (*A*) three or (*C*, *E*–G, and *J*) two independent experiments. (*A*–*C* and *E*–*I*) Experiments were blinded. $^{**}P < 0.01$ (unpaired two-tailed *t* test with Holm–Sidak correction).

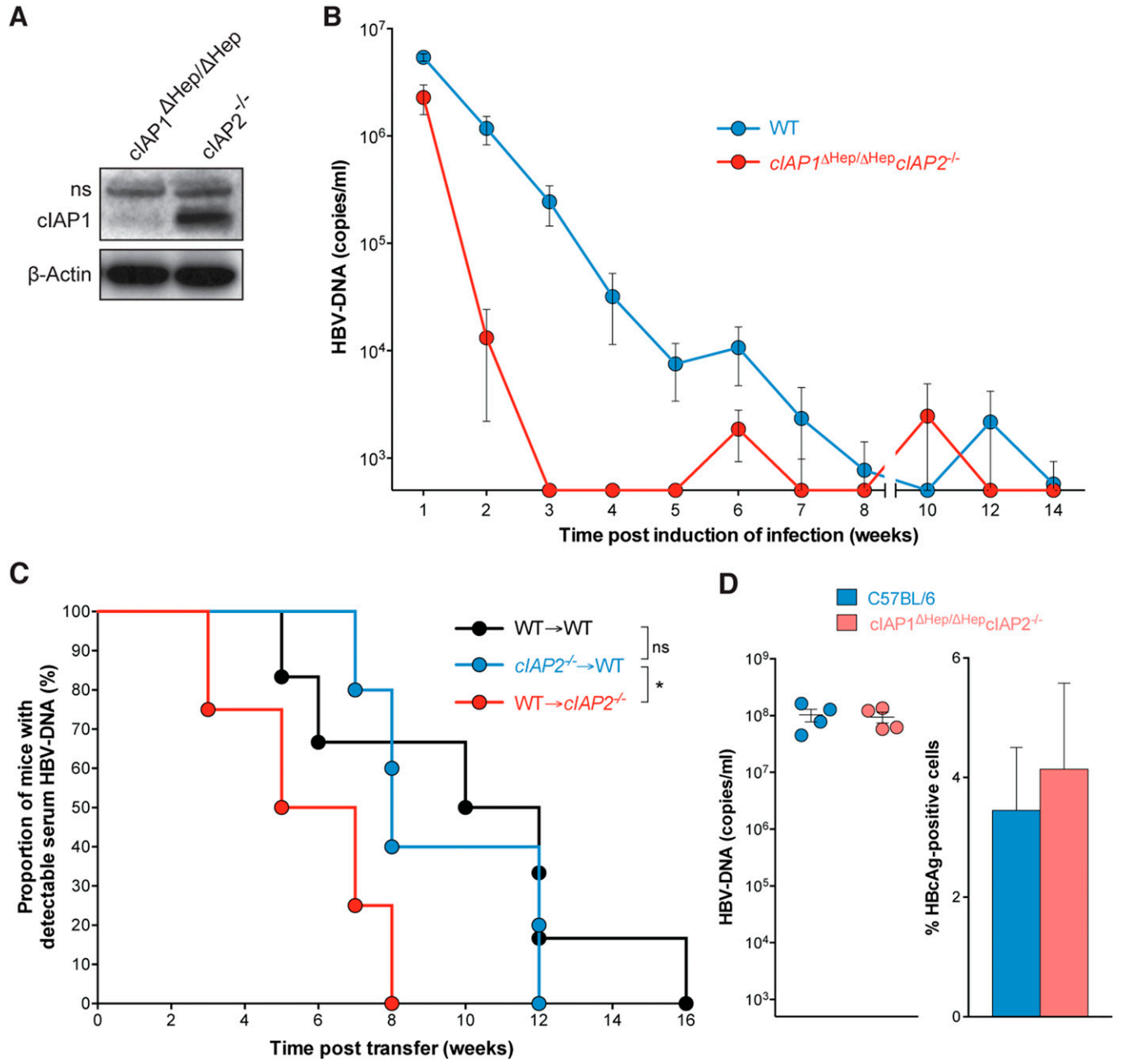

Fig. S3. Mice deficient in cIAPs are fully susceptible to HBV infection but rapidly control HBV DNA levels. (*A*) Western blot analysis showing liver protein levels of cIAP1 in mice with a liver-specific conditional deficiency of cIAP1 and mice with a total deficiency of cIAP2. ns, nonspecific band. (*B*) Serial measurement of serum HBV DNA levels in mice of the indicated genotype after induction of HBV infection ($n = 5–8$ in each group). (*C*) Proportion of animals and time when chimeras (the hemopoietic tissue genotype left of the arrow was transferred into recipients with the genotype indicated right of the arrow) first achieved an undetectable serum HBV DNA level ($n = 4–6$ for each group). ns, not significant. (*D*) Serum HBV DNA levels and proportion of HBcAg-expressing hepatocytes in mice of the indicated genotype 3 d after induction of infection ($n = 4$ per group). (*B* and *D*) Graphs show means and SEMs, and data are representative of two independent experiments. Experiments were blinded. $^*P < 0.05$ (log-rank Mantel–Cox test).

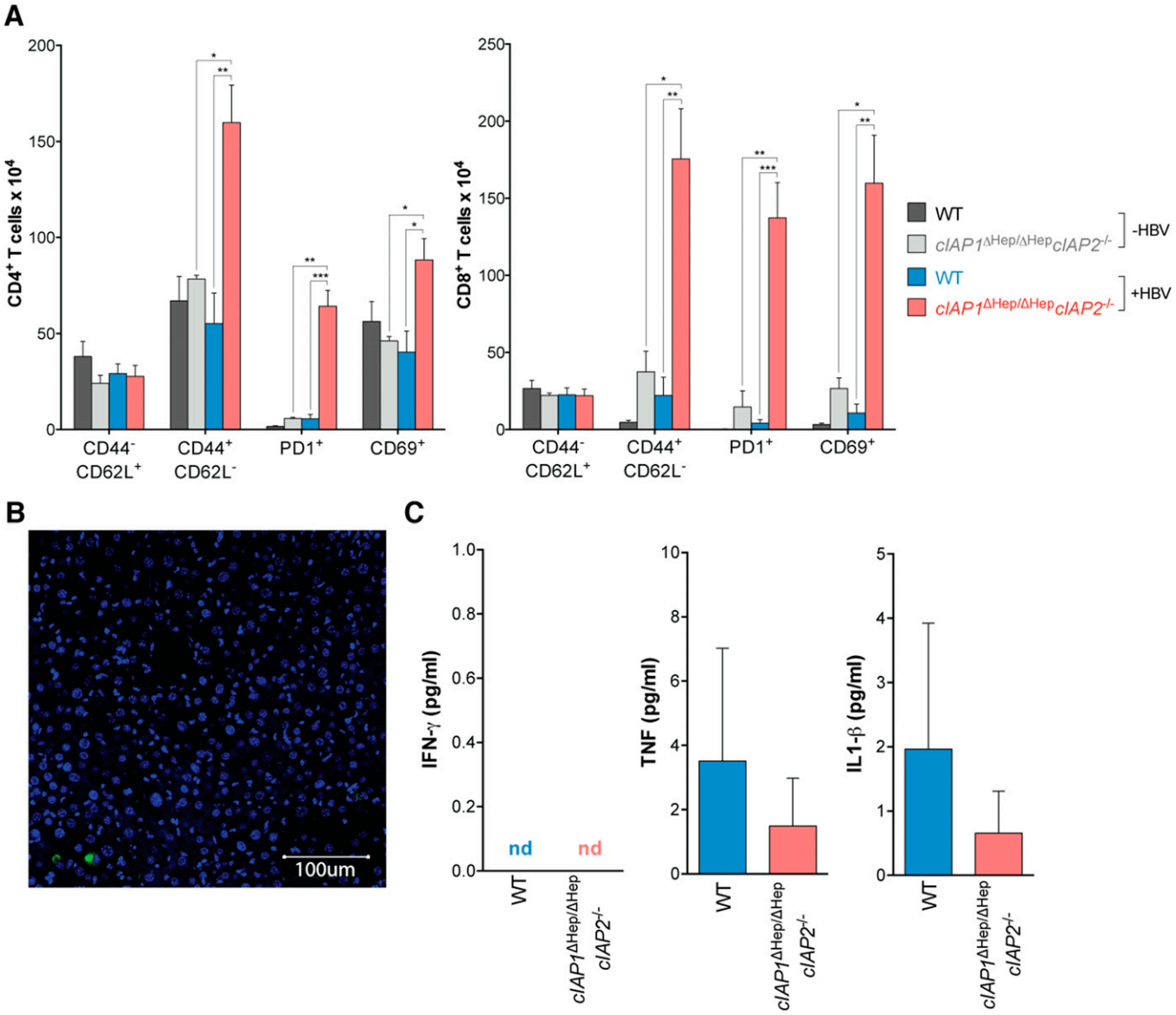

Fig. S4. Immune responses in cIAP gene-targeted mice after induction of infection. (*A*) Fluorescent cell-sorting quantification of T-cell populations infiltrating the livers of uninfected or HBV-infected mice with the indicated genotypes 2 wk after induction of infection ($n = 5$ in each group). (*B*) Immunofluorescence staining (blue, DAPI; green, TUNEL) of liver sections from 7-wk-old uninfected cIAP-deficient mice. (*C*) Quantification of serum cytokine levels 16 d after induction of HBV infection in mice of the indicated genotypes ($n = 5$ in each group). (*A* and *B*) Graphs show means and SEMs, and data are representative of three independent experiments. (*A* and *C*) Experiments were blinded. $CD44^{-}CD62L^{+}$, naïve T cells; $CD44^{+}CD62L^{-}$, activated T cells; $CD69^{+}$, acutely activated T cells; nd, not detected; $PD1^{+}$, repeatedly activated T cells. $^{*}P < 0.05$; $^{**}P < 0.01$; $^{***}P < 0.001$ (unpaired two-tailed *t* test with Holm–Sidak correction).